energies

MDPI

Article

Design and Optimization on the Degree of Hybridization of Underground Hybrid Electric Trackless Rubber-Tyred Vehicle

Xiaoming Yuan [1,2,3], Yao Lu [1], Jiusheng Bao [1,*], Peixin Han [1], Yan Yin [1] and Xu Wang [1]

[1] School of Mechatronic Engineering, China University of Mining and Technology, Xuzhou 221116, China
[2] China Coal Technology & Engineering Group Taiyuan Research Institute Co., Ltd., Taiyuan 030006, China
[3] China National Engineering Laboratory for Coal Mining Machinery, Taiyuan 030006, China
* Correspondence: cumtbjs@cumt.edu.cn; Tel.: +86-138-1345-1343

Abstract: The explosion-proof diesel engine trackless rubber-tyred vehicle (TRTV) has the disadvantages of high fuel consumption and serious exhaust emissions, while the problems of insufficient power and short endurance limit the development of the explosion-proof battery trackless rubber-tyred vehicle. Hybrid technology can effectively reduce fuel consumption and emissions on the basis of ensuring sufficient power. Exploring the application of hybrid electric trackless rubber-tyred vehicle (HETRTV) has practical significance for coal mine auxiliary transportation. The degree of hybridization (DOH) will directly affect the performance and cost of TRTV, which needs to be focused in the development process. The effects of DOH on dynamic performance, fuel economy, emission performance, and cost were studied based on a simulation by ADVISOR, and the results were verified and analyzed by experiment. Compared with the flameproof diesel engine trackless vehicles, HETRTV with the optimal DOH exhausts has far less gas emissions. The engine fuel consumption and the equivalent fuel consumption of the vehicle are reduced by 33.9% and 12.5%, respectively. The results showed that in spite of a small increase in cost, the HETRTV with the optimal DOH can not only meet the driving requirements of underground working conditions but also greatly improve fuel economy and emission performance.

Keywords: trackless rubber-tyred vehicle (TRTV); hybrid technology; degree of hybridization (DOH); ADVISOR; secondary development; multi-objective optimization

Citation: Yuan, X.; Lu, Y.; Bao, J.; Han, P.; Yin, Y.; Wang, X. Design and Optimization on the Degree of Hybridization of Underground Hybrid Electric Trackless Rubber-Tyred Vehicle. *Energies* **2022**, *15*, 6544. https://doi.org/10.3390/en15186544

Academic Editor: Mario Marchesoni

Received: 4 August 2022
Accepted: 2 September 2022
Published: 7 September 2022

1. Introduction

The trackless rubber-tyred vehicle (TRTV) is a highly efficient underground auxiliary transportation equipment in coal mines, which could be divided into flameproof diesel engine type and flameproof battery type by power source. The existing flameproof diesel engine TRTV is characterized by high energy consumption and serious pollution [1,2], while the flameproof battery TRTV features insufficient power and poor endurance. However, hybrid technology is a relatively mature environmental protection and energy saving technology which can effectively achieve better fuel economy and emission performance on the basis of ensuring vehicle dynamic performance [3]. Developing the research on a hybrid electric trackless rubber-tyred vehicle (HETRTV) will be of great significance to efficient and environmentally friendly transportation within the mines.

The degree of hybridization (DOH) [4–6] is an important parameter reflecting the matching degree of engine and motor in hybrid power system. It has a direct influence on both the performance and cost of TRTV, which makes it a focus of attention in the design and development process. At present, researchers have done some research on the DOH, however, mainly focused on hybrid buses, coaches, and other commercial vehicles. For example, Zeng and Cui put forward the design method of DOH of a parallel hybrid electric vehicle, and studied the relationship between hybrid degree and the economic benefit, cost-return period of the whole vehicle [6,7]. Xia took a parallel hybrid electric city bus as

the research object and studied that kind of city bus's power assembly [8]. Taking series hybrid commercial vehicle as the research objects, Hu conducted the study on the design of characteristic parameters that were centered on the DOH and made a simulation by means of MATLAB [9]. However, there are few studies on HETRTV, and the existing literature is limited to feasibility analysis, driving form exploration, system structure design, etc.

Therefore, this paper aims to improve the fuel economy of TRTV, reduce exhaust emissions and manufacturing costs, and design and study the DOH of HETRTV. The HETRTV that is based on the optimal DOH design can meet the driving requirements of underground working conditions. Compared with the explosion-proof diesel engine trackless rubber-tyred vehicle, the performance of the vehicle has been greatly improved, and the power performance and fuel economy of the vehicle have also been greatly improved. Therefore, the design and research of DOH for the design, manufacture, and use of HETRTV have important guiding value and practical significance.

2. Main Components Selection and Parameter Design

This paper refers to WCQ-3B explosion-proof diesel TRTV for the design of HETRTV. The WCQ-3B explosion-proof diesel TRTV is one of the main models of auxiliary transportation in coal mines. It is an underground trackless transportation machinery that is driven by an explosion-proof diesel engine and adopts a hinged frame, mechanical transmission, and four-wheel drive. It is mainly used for underground transportation in coal mines with a roadway section of not less than 9 m^2 and a slope of not more than 14°.

In this paper, the design of the power system parameters of HETRTV is mainly based on the determination of the structure type of the whole vehicle driving system. Considering the working conditions, fuel economy, technical maturity, development and maintenance costs, and other factors, this paper selects the single shaft parallel type as the layout of the HETRTV drive system. Figure 1 is a schematic diagram of the drive system of the hybrid trackless rubber-tyred vehicle. According to the essential parameters of WCQ-3B type TRTV, the parameters of various power components (engine, motor, battery, main reducer transmission, etc.) are reasonably designed and calculated.

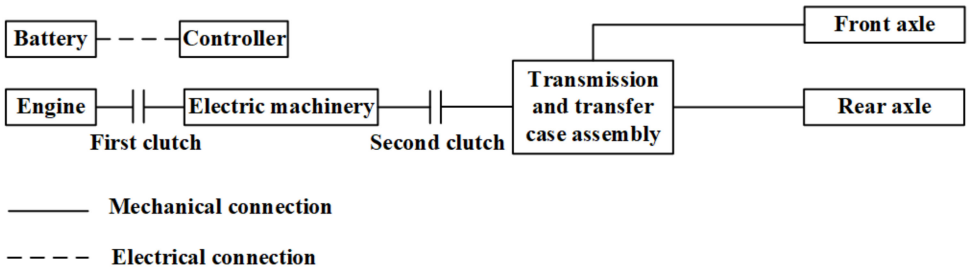

Figure 1. Schematic diagram of drive system of HETRTV.

Among all kinds of factors affecting the fuel economy of hybrid electric vehicles, the proportion of DOH is the largest, and fuel economy is less affected by battery capacity, main deceleration ratio, and voltage level [7]. Therefore, to avoid repeated calculation of parameters in the simulation when studying the influence of DOH on the performance of TRTV, all parameters except DOH remain unchanged [10].

According to *The General Technical Condition of the Flameproof Diesel Vehicle with the Rubber Wheels for the Mine (MTT989-2016)* and combined with the general indexes of road vehicles, the performance requirements of HETRTV are formulated as shown in Table 1.

The total power that is provided by TRTV must meet the vehicle performance requirements of the vehicle performance target. According to the vehicle dynamics theory, the total power that is required by the vehicle includes the steady-state power and transient power that is generated by overcoming rolling resistance, slope resistance, wind resistance, and acceleration resistance [11]. According to the calculation theory of hybrid electric vehicles and the characteristics of TRTV components, the power system parameters of HETRTV are designed [12].

Table 1. Performance requirements of HETRTV.

Dynamic Performance	Indicator Requirements
Maximum speed (km·h^{-1})	≥40
Maximum grade at 7 km·h^{-1} (%)	≥25
Continuous climbing speed on 3% slope (km·h^{-1})	20
Acceleration time of 0–20 km·h^{-1} (s)	≤6
Fuel consumption (%)	Reduce by over 25

Select the engine and motor according to the actual working conditions and performance requirements. The lead-acid battery has the advantages of low price, high safety performance, and low maintenance cost. In this paper, the lead-acid battery is used as the storage battery of HETRTV [13]. Design the battery parameters according to the DOH range (0.1~0.5) and the maximum power of the motor. According to the maximum speed and maximum gradient requirements under different operating modes [12], calculate the transmission ratio of the final drive and the gearbox, as shown in Table 2.

Table 2. Power system parameters for HETRTV.

System Components	Component Types	Parameters
Engine	Flameproof diesel engine	\
Motor	Flameproof permanent magnet motor	\
Battery	Flameproof lead-acid battery	25 × 100 A·h
Final drive	\	Ration: 10.6
Gearbox	\	Ratio: 5.534, 3.111, 1.73, 1, 0.818
Control strategy	Electrically assisted control	\

For the HETRTV, the total power is provided by the engine and the motor. This chapter only calculates the total power that is required by the hybrid power system, while the power calculation of the engine and the motor, i.e., the design of the degree of mixing, will be calculated and optimized in detail later.

3. Secondary Development of ADVISOR for TRTV

3.1. Building Modules

In this paper, the flameproof diesel engine and permanent magnet motor is modelled by an experimental method, and the test bench for HETRTV is shown in Figure 2. The bench employs a uniaxle parallel connection mode, and flameproof diesel engine and permanent magnet motor are arranged in a coaxial way. It can carry out three model experiments with flameproof diesel engine drive, permanent magnet motor drive, and hybrid drive, respectively.

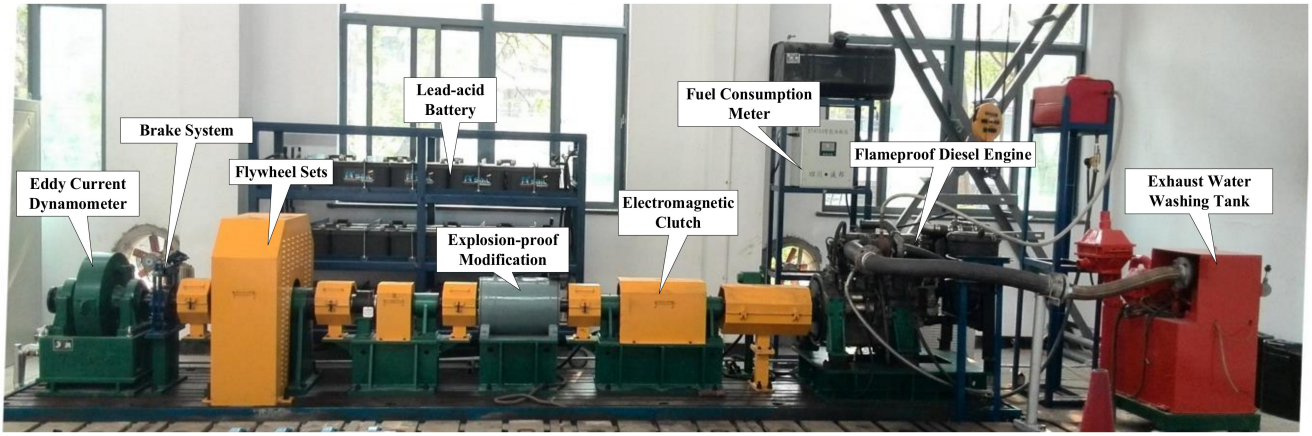

Figure 2. Hybrid test bench for HETRTV.

3.1.1. Flameproof Diesel Engine Module

The characteristics of the KC4102ZDFB flameproof diesel engine were tested on the test bench. In terms of the experimental data, the flameproof diesel engine module was established and imported into ADVISOR software.

The main model parameters of the flameproof diesel engine are shown in Table 3.

Table 3. Main model parameters of the flameproof diesel engine.

Projects	Numerical Values
Speed range ($r \cdot min^{-1}$)	1000~2400
Torque range (N·m)	0~300
Fuel consumption rate ($g \cdot kWh^{-1}$)	Experimental data
HC ($g \cdot s^{-1}$)	Experimental data
CO ($g \cdot s^{-1}$)	Experimental data
NOx ($g \cdot s^{-1}$)	Experimental data
Maximum torque ($N \cdot m^{-1}$)	Experimental data

The external characteristic curves and universal characteristic curves of KC4102ZDFB-type flameproof diesel engine are shown in Figures 3 and 4, respectively.

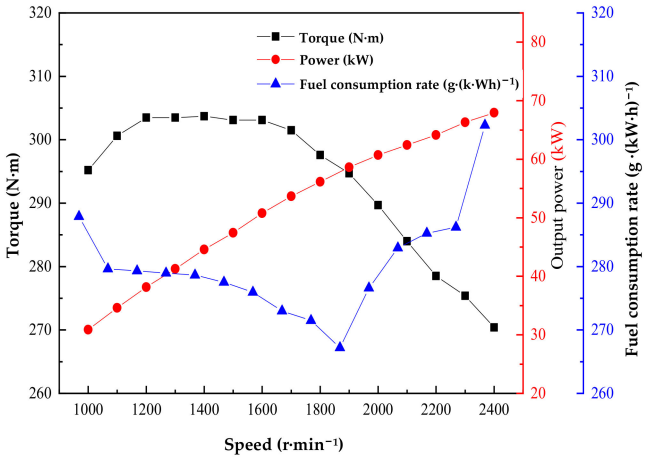

Figure 3. External characteristic curves of KC4102ZDFB-type flameproof diesel.

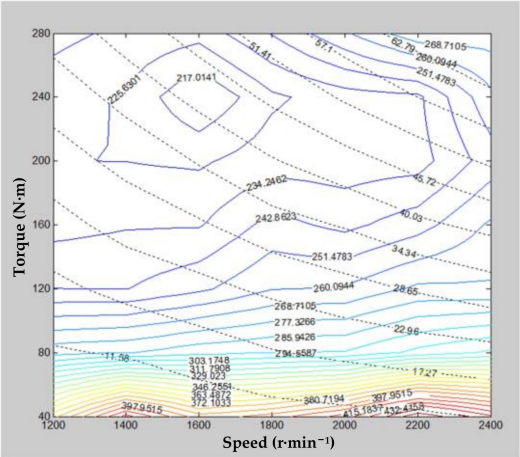

Figure 4. Characteristic performance curves of KC4102ZDFB-type flameproof diesel engine.

The exhaust emission test and the universal characteristic test of the flameproof diesel engine were implemented at the same time. The harmful exhaust of HC, CO, and NOx were

collected from the test rig. The volumetric concentrations of HC, CO, and NOx emissions are shown in Figures 5–7, respectively.

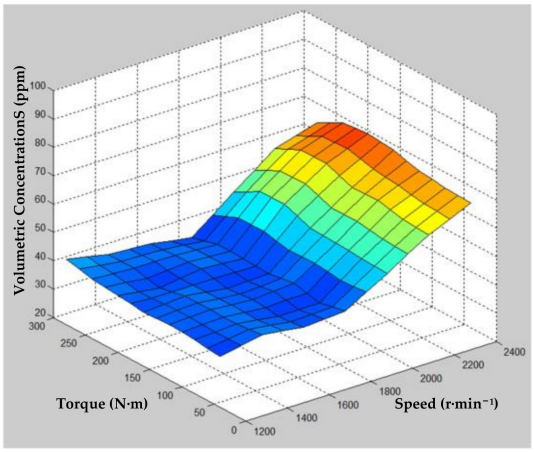

Figure 5. Three dimensional map of the HC volume concentration.

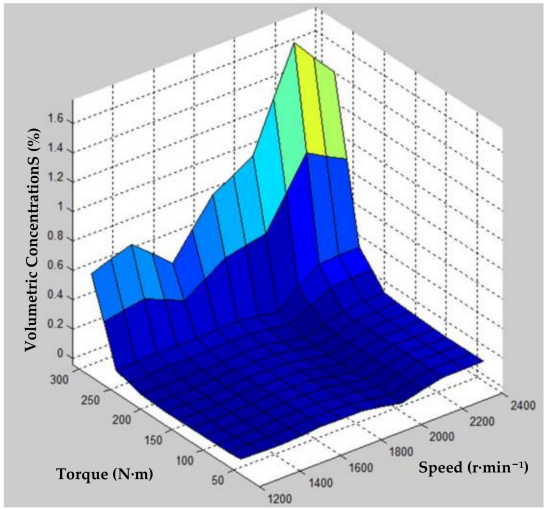

Figure 6. Three dimensional map of the CO volume concentration.

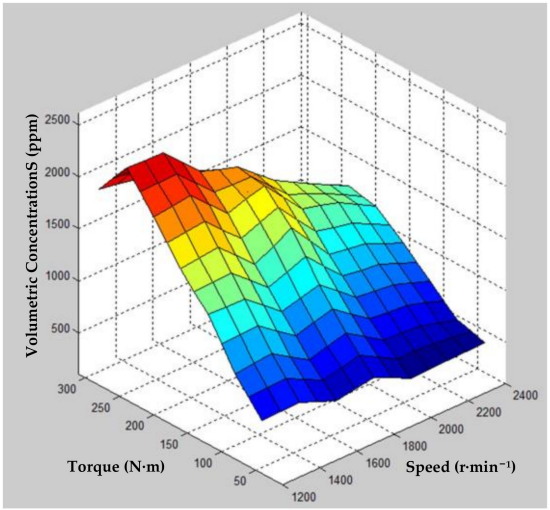

Figure 7. Three dimensional map of the NOx volume.

Through the external characteristic test, universal characteristic test, and exhaust emission test of the explosion-proof diesel engine, the data that are required for the experimental modeling of the explosion-proof diesel engine are obtained, thus the explosion-proof diesel engine module of ADVISOR software can be established [14].

3.1.2. Flameproof Permanent Magnet Motor Module

The relevant data of YGDLB flameproof permanent magnet motor were measured on the test bench, including the motor speed range, torque range, motor efficiency, and motor quality. According to the experimental data, the flameproof permanent magnet motor module is established and imported into ADVISOR software. The permanent magnet motor experimental modeling mainly involves parameters which are shown in Table 4.

Table 4. Parameters of the permanent magnet motor.

Projects	Speed Range ($r \cdot min^{-1}$)	Torque Range ($N \cdot m$)	Motor Efficiency (%)	Motor Quality (kg)
Numerical values	0~2400	−160~160	Experimental data	216

Figures 8 and 9 are two dimensional and three dimensional efficiency curves of YGDLB flameproof permanent magnet motor, respectively.

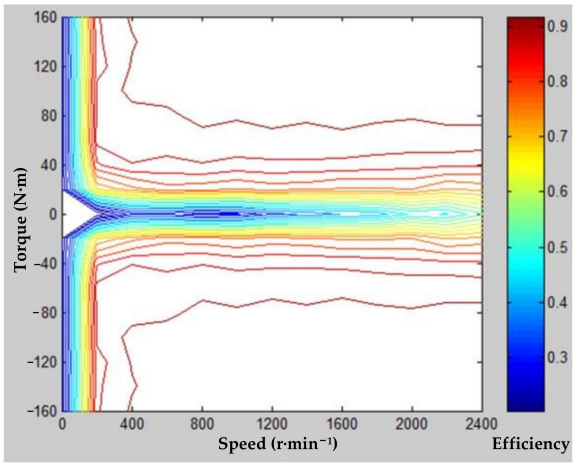

Figure 8. Two dimensional curves of efficiency.

It can be seen from Figures 8 and 9 that when the motor torque is less than 40 N·m, the efficiency of the permanent magnet motor is not greater than 0.8. In the range of 40~160 N·m, the efficiency fluctuates slightly between 0.8 and 1.0. When the torque is greater than 40 N·m, the efficiency is almost stable under different rotational speeds and the same torque. The explosion-proof permanent magnet motor can achieve the maximum torque output from the low-speed stage, while the fuel economy of the explosion-proof diesel engine is poor in the idle stage, so the explosion-proof permanent magnet motor has obvious advantages in the low-speed operation stage.

Through the motor efficiency test of flameproof permanent magnet motor, the data needed for the experimental modeling of flameproof permanent magnet motor are obtained. By modifying the original motor module program in ADVISOR software, the flameproof permanent magnet motor module of ADVISOR software can be established.

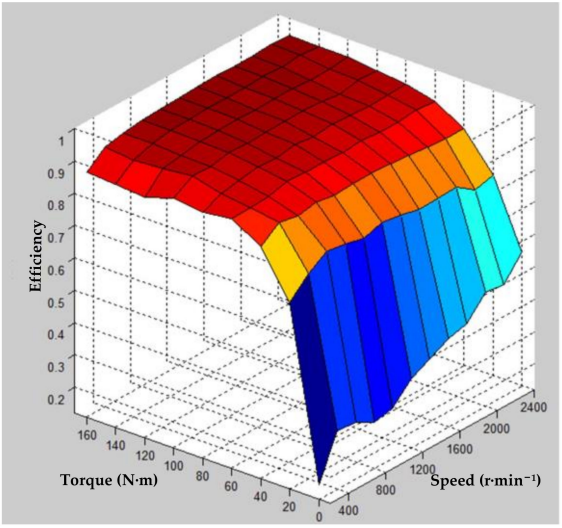

Figure 9. Three dimensional curves of efficiency.

3.2. Driving Cycle Model

For the time being, there are few studies on the underground road driving cycle of the coal mine. This paper combines the CYC_KS driving cycle with the CYC_JX driving cycle to form the CYC_WCQ driving cycle. In the later simulation, the CYC_WCQ driving cycle serves as the driving cycle of TRTV and the operation conditions for determining the optimal DOH. The CYC_KS is a part of the road driving cycle of an underground tramcar in document [15]. The measured data are close to the running driving cycle of TRTV, but on account of the lack of slope information, the climbing ability of TRTV cannot be tested.

CYC_JX that is formulated according to *The General Technical Condition of the Flameproof Diesel Vehicle with the Rubber Wheels for the Mine (MTT989-2016)* is a limit driving cycle of TRTV. This driving cycle works as a good choice to test whether the dynamic performance of TRTV meets the requirements. However, it is also too complex, which is not in line with the actual running conditions of TRTV. The CYC_WCQ driving cycle has the characteristics of the above two driving cycles and is close to the actual working condition TRTV. The driving cycle is shown in Figure 10.

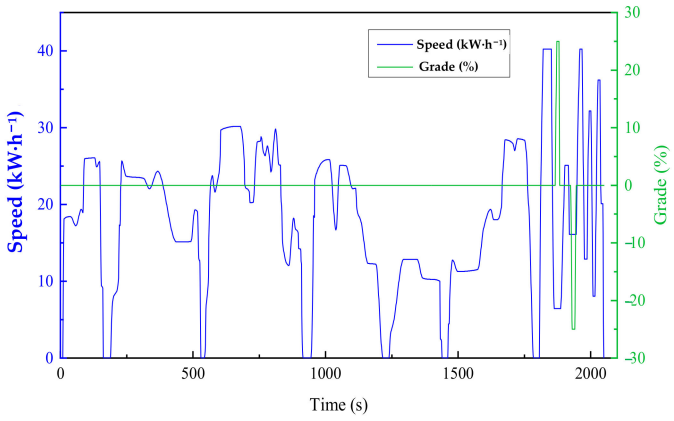

Figure 10. CYC_WCQ driving cycle.

4. Effects Analysis of DOH for HETRTV

DOH refers to the percentage of motor power to the total power of the power source, and its expression can be written as follows:

$$R = \frac{P_{\mathrm{m}}}{P_{\mathrm{m}} + P_{\mathrm{e}}} = \frac{P_{\mathrm{m}}}{P} \tag{1}$$

where R is the degree of hybridization; P_m is the rated power of engine, kW; and P_e is the rated power of electrical machinery, kW.

The HETRTV that is designed in this paper adopts the electric booster type, with the engine as the main power source and the motor as the auxiliary power source. Therefore, the range of DOH is 0.1~0.5.

4.1. Effects of DOH on Dynamic Performance

4.1.1. Effects of DOH on Vehicle Curb Mass

The change of the vehicle curb mass has a great influence on the vehicle dynamic performance [16], therefore, studying the change of the curb mass of TRTV with DOH is needed. As the battery capacity has little effect on the properties of TRTV, the vehicle curb mass under different DOH was compared with the battery of the same capacity during performance simulation. The change of vehicle curb mass with DOH is shown in Figure 11.

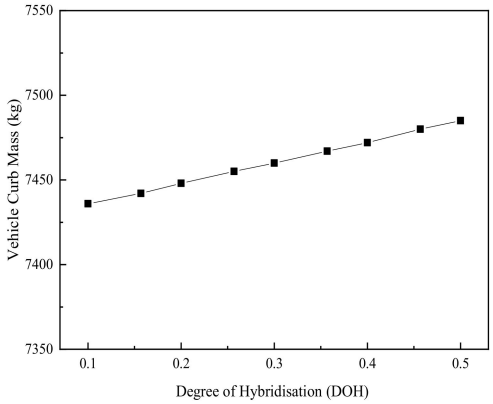

Figure 11. Figure caption curve of vehicle curb mass with degree of hybridization.

It can be seen that when the DOH is in the range of 0.1~0.5, the vehicle curb mass increases by about 50 kg, roughly 0.7% of the total vehicle curb mass from Figure 10. Therefore, in the process of performance simulation, the influences on power performance, fuel economy, and emission performance of TRTV that are exerted by the vehicle curb mass can be neglected.

4.1.2. Effects of DOH on Acceleration Time, Maximum Speed, and Grade

The dynamic performance of HETRTV is mainly measured from three aspects: acceleration performance, maximum speed, and grade. In the simulation, the acceleration time from 0 to 20 km·h^{-1} represents the acceleration performance of TRTV, and the climbing speed is set at 7 km·h^{-1}. The CYC_WCQ working condition is selected for the simulation. The simulation results are shown in Figures 12–14.

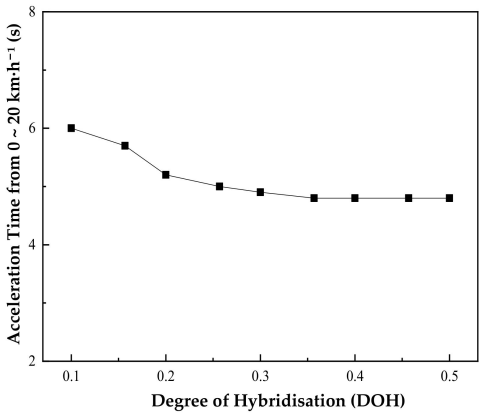

Figure 12. Curves of acceleration time with DOH.

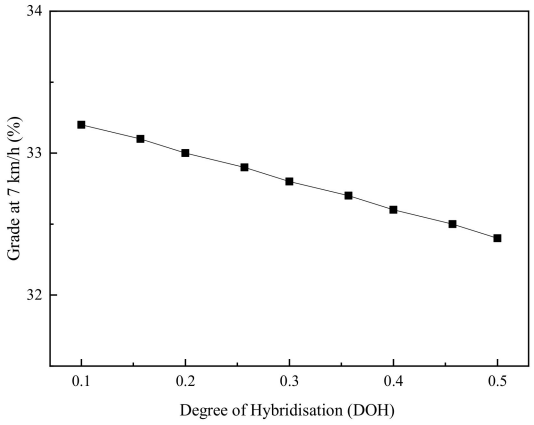

Figure 13. Curves of maximum grade at 7 km·h^{-1} with DOH.

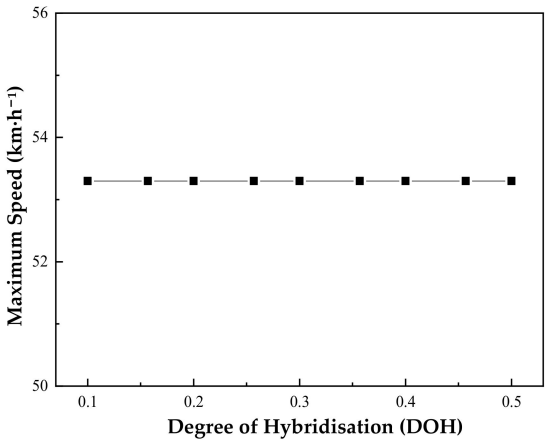

Figure 14. Curves of maximum speed with DOH.

From Figures 12–14, it can be seen that in the range of DOH from 0.1 to 0.5, the acceleration time from 0 to 20 km·h^{-1}, the maximum grade at 7 km·h^{-1} and the maximum speed change of TRTV all have little changes, which all indicates that the change of DOH has little effect on the power performance.

4.2. Effects of DOH on Fuel Economy

Nowadays, the fuel economy simulation of hybrid electric vehicles mostly takes the fuel consumption per 100 km of engine as the fuel economy evaluation index, without considering the change of the battery energy. In this paper, the concept of battery equivalent fuel consumption is introduced to express the sum of engine fuel consumption and battery equivalent fuel consumption, and it is used as the ultimate basis for the study of fuel economy of HETRTV. According to *Test methods for energy consumption of heavy-duty hybrid electric vehicles (GB/T 19754-2015)*, the equivalent fuel consumption of the battery can be figured out by formula (2):

$$V_{\text{fuel}} = \frac{E_{\text{k}}}{D_{\text{fuel}} Q_{\text{fuel}-\text{low}} \eta_{\text{eng}}} \tag{2}$$

where V_{fuel} is the equivalent fuel consumption of the battery, L; D_{fuel} is the diesel density, 0.85 g·cm^{-3}; $Q_{\text{fuel-low}}$ is the low heat of diesel combustion, 43,000 kJ·kg^{-1}; and η_{eng} is the average working efficiency of engine, set at 0.4.

The simulation is carried out under the CYC_WCQ driving cycle, and the relationship between DOH and fuel economy of HETRTV is studied by using engine fuel consumption, battery equivalent fuel consumption, as well as the vehicle equivalent fuel consumption that is represented by the sum of the two. The results are shown in Figures 15–17.

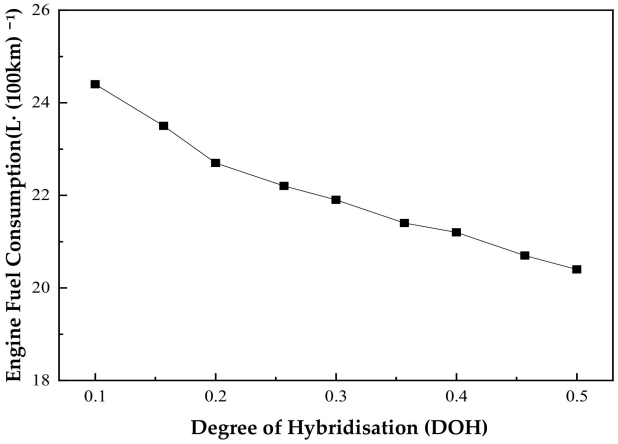

Figure 15. Curves of the engine fuel consumption with DOH.

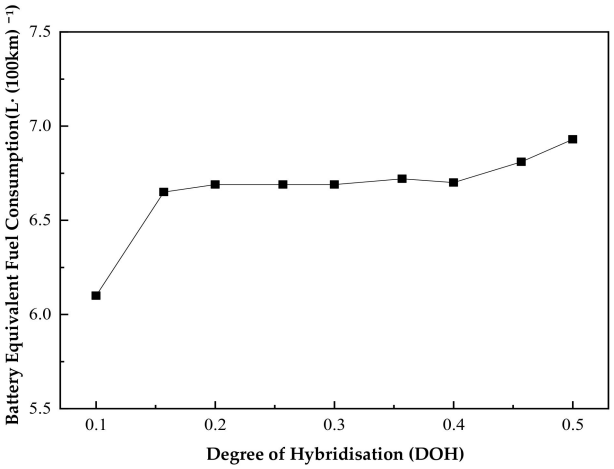

Figure 16. Curves of the battery equivalent fuel consumption with DOH.

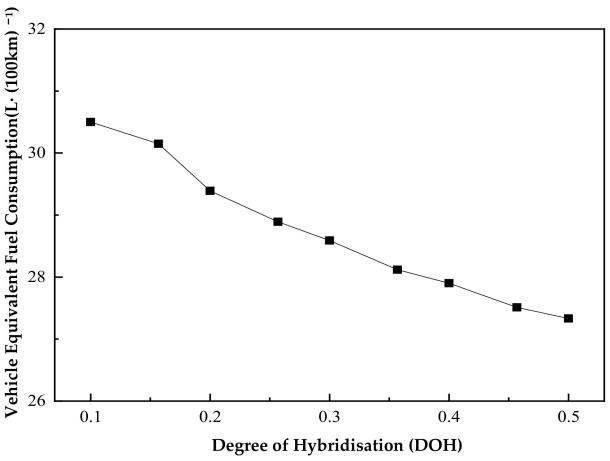

Figure 17. Curves of the equivalent fuel consumption with DOH.

It can be seen that both the engine fuel consumption and the vehicle equivalent fuel consumption of HETRTV present a downward trend with the increase of DOH, while the battery equivalent fuel consumption shows an upward trend with the increase of DOH, but the overall change is not apparent. The simulation results of the vehicle equivalent fuel consumption reveals that the increase of DOH is beneficial to improving the fuel economy

of TRTV. The fitting method is used by SPSS (Statistical Product Service Solutions) software to study the relationship between the vehicle equivalent fuel consumption and DOH:

$$f_1(R) = 14.459R^2 - 18.075R + 25.925 \quad (3)$$

where R is the DOH, which ranges from 0.1 to 0.5; and $f_1(R)$ is objective function of the equivalent fuel consumption of HETRTV, L·(100 km)$^{-1}$.

4.3. Effects of DOH on Exhaust Emission

Figure 18 shows the variation curve of exhaust emission with DOH under the CYC_WCQ driving cycle. The simulation results are expressed by specific emission (g·km^{-1}).

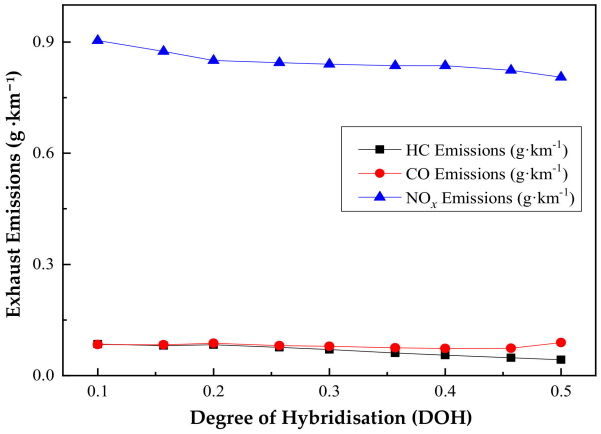

Figure 18. Curves of emission with DOH.

As can be seen from Figure 18, the emission of NOx under the CYC_WCQ driving cycle is significantly higher than that of HC and CO. Analysis of the simulation data suggests that the HC and NOx emissions are in a downward trend with the increase of DOH, and the emissions lessened. The change of CO emission is slightly complex, it goes down on the whole, but it rises back up in the hybridization stage. The relationships between HC, CO, and NOx and DOH are obtained by fitting:

$$f_2(R) = -0.15R^2 - 0.023R + 0.09 \quad (4)$$

$$f_3(R) = 2.485R^3 - 2.05R^2 + 0.472R + 0.053 \quad (5)$$

$$f_4(R) = -5.219R^3 + 5.085R^2 - 1.683R + 1.028 \quad (6)$$

where $f_2(R)$ is the objective function of HC emissions, g·km^{-1}; $f_3(R)$ is the objective function of CO emissions, g·km^{-1}; and $f_4(R)$ is the objective function of NOx emissions, g·km^{-1}.

4.4. Effects of DOH on Manufacturing Cost

Compared with flameproof diesel TRTV, the HETRTV costs more in light of manufacturing, and the costs change mainly in batteries, motors, controllers, engines, and other costs. The added cost of HETRTV can be calculated by following formula:

$$\Delta C = C_b + C_m - C_e + C_s \quad (7)$$

where ΔC is the objective function of increased cost of HETRTV, RMB; C_b is the cost of lead-acid batteries, RMB; C_m is the cost of permanent magnet motors (including controllers), RMB; C_e is the reduced cost of flameproof diesel engines, RMB; and C_s is the additional cost of HETRTV system, set at 8000 RMB.

4.4.1. Battery Cost Analysis

In order to obtain the relationship between the capacity and price of domestic lead-acid batteries, this paper investigates the prices of two well-known manufacturers Aa and B lead-acid batteries in the market, and the prices can reflect the general prices of domestic lead-acid batteries. The price comparison chart is shown in Figure 19.

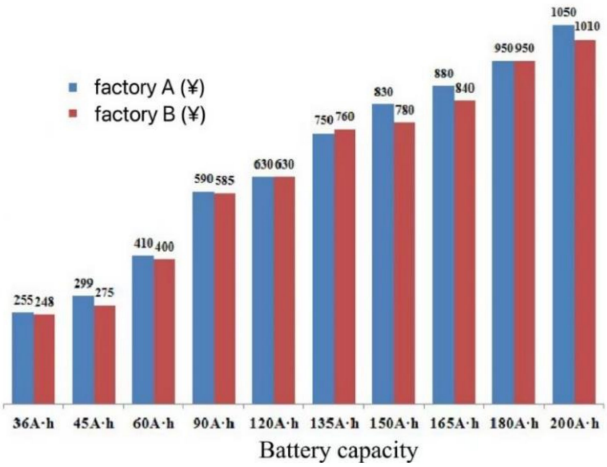

Figure 19. Price comparison charts of manufacturer A and manufacturer B.

The price difference between the two batteries is within 8%. As the price difference between the two batteries is not large, this paper selects manufacturer A for cost research and uses SPSS software to perform linear regression on its capacity and price. The regression equation is fitted by SPSS as follows:

$$C_{b1} = 4.73C + 106 \tag{8}$$

where C_{b1} is the price of monomer lead-acid battery with specific capacity and C is the battery rated capacity, A·h.

The relationship between the cost of newly added lead-acid batteries and the DOH of HETRTV can be worked out as follows:

$$C_b = 25C_{b1} = 22,940R + 2650 \tag{9}$$

4.4.2. Motor Cost Analysis

According to the relevant literature [17,18], the formula for calculating the cost of a hybrid electric vehicle motor and controller is as follows:

$$C_m = A + BP_m \tag{10}$$

where A and B are the fitting coefficients, which are obtained by the linear fitting of the known motor power price.

The costs of the engine/transmission and electric motor/electronics are calculated from the maximum power rating of the components and their unit cost ($/kW) [19,20]. Through consulting the relevant literature and calculation, set the values of A and B as 3000 RMB and 180 RMB, respectively. The relationship between the cost of a newly added permanent magnet motor and the DOH of HETRTV can be worked out as follows:

$$C_m = 3000 + 12,600R \tag{11}$$

4.4.3. Engine Cost Analysis

The price of each power of diesel engine is generally 200~320 RMB, mostly 260~290 RMB. The reduced cost of the engine can be worked out finally as follows:

$$C_e = 19,600R \tag{12}$$

Based on the above cost calculation and analysis results and substituting into formula (7), the cost difference calculation method of HETRTV and flameproof diesel TRTV can be obtained, and the objective function of increased cost of HETRTV can be obtained as follows:

$$f_5(R) = \Delta C = 15,940R + 13,650 \tag{13}$$

It can be seen that the increased cost of HETRTV increases with the increase of DOH.

5. Simulation and Experiment

The optimization of DOH of HETRTV involves many objectives, such as power performance, fuel economy, emission performance, and cost, and it is a typical multi-objective optimization problem. In many cases, there may be conflicts among sub-objectives, which cannot ensure that all the objectives are achieved at the same time. In order to achieve the optimal DOH, these objectives must be optimized at the same time.

5.1. Determination of Optimal DOH

This paper adopts the genetic algorithm [17–19,21] that is based on the objective weighting method, which means that the multi-objective optimization problem of HETRTV is transformed into a single objective optimization problem by the weight coefficient transformation method, and the DOH is taken as a single design variable, thus the optimal DOH of HETRTV is obtained. The optimization process mainly comprises the establishment of objective function, determination of the weight coefficient, and optimization.

5.1.1. Establishing Objective Function

In this paper, the DOH is taken as a single design variable, and the dynamic performance such as acceleration time, maximum speed, and grade are taken as constraints. The objective function is characterized by the equivalent fuel consumption, the emissions, and the increased cost of HETRTV. Therefore, the design requirements of this multi-objective optimization problem are as follows:

(1) Objective function:

$$\min F(x) = [f_1(R), f_2(R), f_3(R), f_4(R), f_5(R)]$$

(2) Constraints:

$$\text{Acceleration time}: \ t_{0\sim 20\text{km/h}} \leq 6$$

$$\text{Acceleration time}: \ t_{0\sim 20\text{km/h}} \leq 6$$

$$\text{Maximum speed}: \ v_{\max} \geq 40$$

$$\text{Grade at } 7 \text{ km·h}^{-1}: \ i_{\max} \geq 25$$

$$\text{Grade at } 20 \text{ km·h}^{-1} \text{ in engine mode}: \ i \geq 3\%$$

(3) Boundary conditions:

$$0.1 \leq R \leq 0.5$$

The optimization objectives of vehicle equivalent fuel consumption, exhaust emission, and cost have different dimensions, economic meanings, and manifestations, and their effects on

the comprehensive objectives are also different and not comparable with each other. Therefore, the comprehensive evaluation results can only be calculated after dimensionless treatment of the optimization objectives to eliminate the influence of the index dimensions. The objective functions after dimensionless treatment with SPSS by z-score method are as follows [20]:

$$f_1'(R) = 9.065R^2 - 12.65R + 2.828 \quad (14)$$

$$f_2'(R) = -9.514R^2 - 1.448R + 1.449 \quad (15)$$

$$f_3'(R) = 432.375R^3 - 356.671R^2 + 82.129R - 4.753 \quad (16)$$

$$f_4'(R) = -181.34R^3 + 176.699R^2 - 58.484R + 6.314 \quad (17)$$

$$f_5'(R) = 6.325R - 1.897 \quad (18)$$

In this paper, the weight coefficient transformation method is used to transform the multi-objective optimization problem into a single-objective optimization problem by giving weights to each sub-objective function. Therefore, the optimal objective function that was used in this paper can be expressed as follow:

$$F(R) = w_1 f_1'(R) + w_2 f_2'(R) + w_3 f_3'(R) + w_4 f_4'(R) + w_5 f_5'(R) \quad (19)$$

where $f_1'(R)$~$f_5'(R)$ are the objective functions after dimensionless treatment; and w_1~w_5 are the optimal objective weight coefficients.

5.1.2. Determining Weight Coefficients by AHP

This paper uses analytic hierarchy process (AHP) [22–24] to determine the weight coefficient, which mainly includes three parts: hierarchical structure model, judgment matrix, and consistency test.

In this paper, the optimal comprehensive performance of HETRTV is taken as the target layer, and the criterion layer is composed of performance and cost, and equivalent fuel consumption; HC, CO, NOx emissions; and the increased cost of the vehicle constitute the index layer of the model. After the hierarchical structure model is established, the relative importance of each level of evaluation index needs to be qualitatively described. The 1~9 scale method is used to assign the factors of index level and criterion level according to their importance to the upper target level. By using the proportional scale method, the factors of the index level and the criterion level are assigned according to the importance of the upper level targets, so as to construct the comparative judgement matrix A-B of criterion level to target level, the comparative judgement matrix B_1-C_i and B_2-C_i of index level to criterion level. The specific matrices are shown in Table 5.

Table 5. Judgment matrix.

A-B				**B_1-C_i**						**B_2-C_i**		
A	**B1**	**B2**	**w**	**B1**	**C1**	**C2**	**C3**	**C4**	**w**	**B2**	**C5**	**w**
B1	1	2	0.666	C1	1	5	5	5	0.625	C5	1	1
B2	1	2	0.333	C2	1/5	1	1	1	0.125			
				C3	1/5	1	1	1	0.125			
				C4	1/5	1	1	1	0.125			
λmax = 2, CI = 0, RI = 0				λmax = 4, CI = 0, RI = 0.90								
CR = 0 < 0.1				CR = 0 < 0.1								

After the judgment matrix is established, it needs to be checked to ensure the consistency. The judgment matrix must satisfy the consistency requirement. When conducting the consistency test, firstly, the maximum eigenvalue of the judgment matrix is obtained by

MATLAB, and it is substituted into Formulas (20) and (21), so as to calculate the consistency index *CI* and consistency ratio *CR* of the judgment matrix and check its consistency.

$$CI = \frac{\lambda_{\max} - n}{n - 1} \tag{20}$$

$$CR = \frac{CI}{RI} \tag{21}$$

where, n is the degree of the judgment matrix, λ_{max} is the maximum eigenvalue of the judgment matrix, *RI* is the average random consistency index, which can be found from Table 6, *CI* is the consistency index, and *CR* is the consistency ratio of the judgment matrix.

Table 6. Value of average random consistency index.

Degree	**1**	**2**	**3**	**4**	**5**	**6**	**7**	**8**	**9**
RI values	0	0	0.58	0.90	1.12	1.24	1.32	1.41	1.45

The smaller the *CI* value, the higher the consistency of the judgment matrix. When $CI = 0$, the judgment matrix is completely consistent. In general, when $CR < 0.1$, the consistency of the judgment matrix meets the requirements. After calculation, the judgment matrix passed the secondary test. The final weights of each indicator layer are shown in Table 7.

Table 7. Weight coefficient of each indicator layer.

Weights	w_1	w_2	w_3	w_4	w_5
Numerical values	0.416	0.0833	0.0833	0.0833	0.333

The MATLAB Toolbox provides a genetic algorithm toolbox. By setting the parameters in the user interface and calling appropriate functions, the search for an optimal solution set to the objective function can get under way. Table 8 shows the parameters of the genetic algorithm.

Table 8. Parameters setting of genetic the algorithm.

Parameters	**Numerical Values**
Group size	40
Cross probability	0.8
Mutation probability	0.0015
Termination algebra	200

The genetic algorithm introduces the biological evolution principle of "survival of the fittest and survival of the fittest" into the coding tandem population that is formed by the optimization parameters, and screens the individuals according to the selected fitness function and through replication, crossover, and mutation in genetics, so that the individuals with the high fitness are retained and form a new population. The new population integrates the information of the previous generation and is superior to the previous generation. In this way, the fitness of individuals in the population will continue to improve until certain conditions are met, so as to obtain the optimal solution [25,26]. The flow chart of the genetic algorithm is shown in Figure 20.

The MATLAB Toolbox provides a genetic algorithm toolbox. By setting parameters on the user interface and calling appropriate functions, you can search for the optimal solution set of the objective function. The entire interface is composed of three parts: problem step and results, option, and quick reference. In the problem step and results, input the mathematical model of the optimization function that is established above. The number of variables is 1, and the upper and lower limits of variable values are 0.5 and 0.1, respectively. Set the algorithm parameters in option and click start to run. The running results are shown in Figure 21.

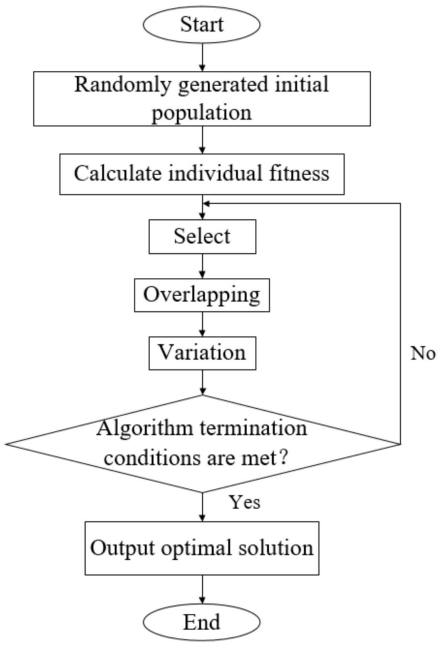

Figure 20. Flow chart of the genetic algorithm.

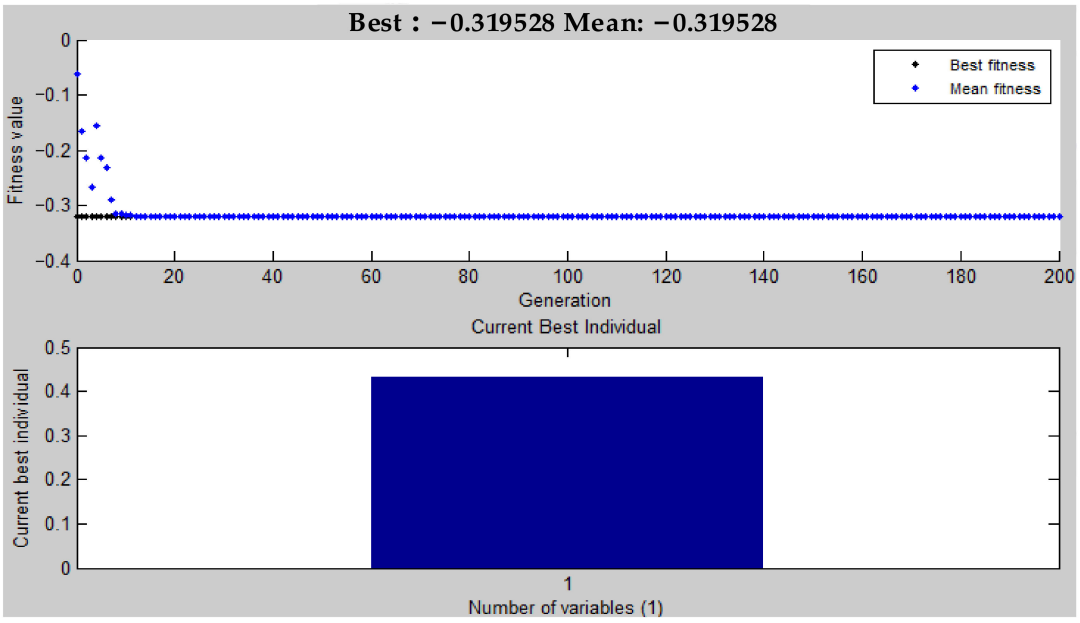

Figure 21. Genetic algorithm iterative result.

By many iterations, it is found that the optimal DOH that is optimized by the genetic algorithm is 0.431. By calculating the results and taking the rounded numbers, the rated powers of engine and motor work out at 40 kW and 30 kW, respectively.

5.2. Comparative Analysis

Whether the design of a hybrid electric vehicle is reasonable depends mainly on whether they can meet the requirements of road conditions under specific conditions. Figure 22 is the simulation result of HETRTV under the CYC_WCQ driving cycle in a coal mine. The simulation results show that the cycle demand speed curves and the simulation speed curves of TRTV almost coincide, which indicates that the HETRTV can meet the requirements under this driving cycle.

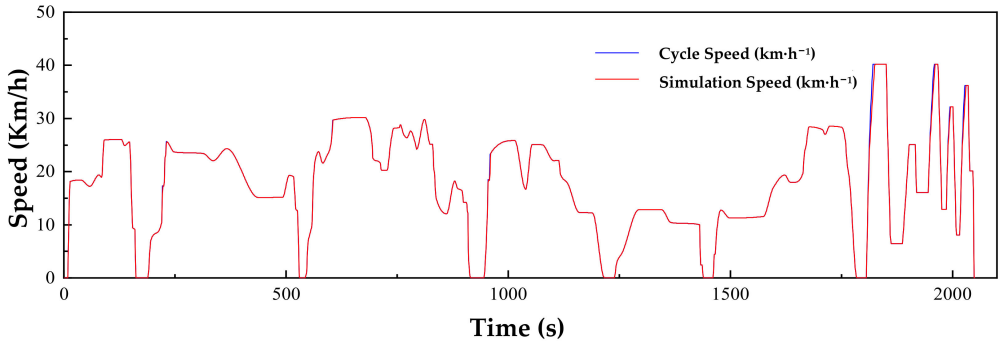

Figure 22. Curves of speed with time under the CYC_WCQ driving cycle.

In order to make an intuitive comparison between the WCQ-3B-type TRTV and HETRTV in the aspect of power performance, fuel economy, and emission performance, the simulation results of WCQ-3B-type TRTV, instead of the actual performance, are used, thus avoiding the errors that are caused by the setting of simulation environment. The simulation results of two vehicles under the CYC_WCQ driving cycle are shown in Table 9.

Table 9. Simulation results of two kinds of trackless rubber-tyred vehicles.

Indexes	WCQ-3B Type	Hybrid Type	Target Values
0–20 km·h^{-1} acceleration time (s)	4.4	4.8	6
Maximum speed (km·h^{-1})	53.3	53.3	40
Maximum grade at 7 km·h^{-1} (%)	33	32.5	25
Maximum grade at 20 km·h^{-1} in Engine Mode (%)	8.2	3.2	3
Engine fuel consumption (L·(100 km)$^{-1}$)	31.6	20.9	≥25% (33.9%)
Equivalent fuel consumption of batteries (L·(100 km)$^{-1}$)	\	6.74	\
Equivalent fuel consumption of vehicle (L·(100 km)$^{-1}$)	31.6	27.64	\
HC emissions (g·km^{-1})	0.088	0.0501	\
CO emissions (g·km^{-1})	0.109	0.07	\
NOx emissions (g·km^{-1})	1.305	0.832	\
0–20 km·h^{-1} acceleration time (s)	4.4	4.8	6
Maximum speed (km·h^{-1})	53.3	53.3	40

Compared with the WCQ-3B-type TRTV, the equivalent fuel consumption of HETRTV under the optimal DOH is reduced by 12.5%. The emissions of HC, CO, and NOx decreased by 42%, 35.8%, and 36.2% respectively. The fuel consumption and exhaust emissions of HETRTV are significantly reduced, and the fuel economy and emission performance improved.

Table 10 shows that the fuel consumption of the engine and the equivalent fuel consumption of the battery are slightly larger than the simulation values. That may be due to some unavoidable interference factors during the test process which make the ideal environment of the simulation impossible. In addition, the battery capacity and voltage level can also exert slight influence on the fuel consumption of the vehicle, thus producing some difference. However, the difference between the simulation and test data is not large, remaining within 7%, which shows that the simulation results are consistent with test results of fuel economy.

In the process of the test, the exhaust emission was recorded continuously. As the unit of exhaust gas that was measured by the exhaust analyzer in the test is volume fraction (ppm, %) and the simulation result is the unit operating mileage emission (g·km^{-1}), the volume fraction that was recorded had first to be converted to unit time mass emission (g·s^{-1}) which was then processed by time integration. Finally, the emission per unit operating mileage was obtained, combining with the distance of 10.14 km. The comparison between the simulation and experiment of exhaust emission is shown in Table 11.

Table 10. Comparison between the simulation and test of fuel economy.

Projects	Engine Fuel Consumption (L·(100 km)$^{-1}$)	Equivalent Fuel Consumption of Batteries (L·(100 km)$^{-1}$)	Equivalent Fuel Consumption of Vehicle (L·(100 km)$^{-1}$)
Simulation	20.9	6.74	27.64
Test	22.3	7.1	29.4
Error (%)	6.7	5.3	6.4

Table 11. Comparison of the simulation and experiment of exhaust emissions.

Projects	HC (g·km^{-1})	CO (g·km^{-1})	NOx (g·km^{-1})
Simulations	0.0501	0.07	0.832
Experiments	0.057	0.078	0.921

From Table 11, it can be seen that the emissions of HC, CO, and NOx are higher than the simulation values. The reason may be that the exhaust performance in the test space has a great influence on the measured concentration and test results of exhaust gas. Although the test bench is at a laboratory that is equipped with fans, exhaust fans, and other equipment for the rapid dilution of exhaust gas, there are still some problems such as the concentration of exhaust gas cannot be diluted in a timely manner, making the exhaust gas concentration stronger. In addition, the unit conversion method will also cause test errors, however, the test values of exhaust emissions are within a reasonable range.

The consistency between the simulation and test results of fuel economy and emission performance shows that the simulation bench of TRTV that is based on ADVISOR software can simulate fuel economy and emission performance accurately, which proves the feasibility of the second development of ADVISOR software, and thus the hybridization design and optimization results that are based on this bench are credible.

6. Conclusions

In this paper, the ADVISOR software has been secondary developed, including the establishment of an explosion-proof diesel engine module, explosion-proof permanent magnet motor module, four-wheel drive module, and TRTV driving cycle, to study the relationship between DOH and HETRTV performance and cost. The multi-objective optimization of the DOH is carried out, and then the simulation and test about the HETRTV are conducted. The research process and results have an important guiding value and practical significance for the design, manufacture, and use of the HETRTV. The main conclusions are as follows:

(1) The secondary development of the ADVISOR software for TRTV is successful by using the secondary developed ADVISOR software to simulate the dynamic performance, fuel economy, and emission performance. The operation is smooth and the data are reasonable.

(2) Through the research on the relationship between the DOH and the performance and cost of underground TRTV, it is found that DOH has little influence on the power performance. Under the underground CYC_WCQ driving cycle, the fuel consumption of the explosion-proof diesel engine and the equivalent fuel consumption of the whole vehicle decreases with the increase of DOH, and the equivalent fuel consumption of the battery increases with the increase of DOH, but the change is small; The exhaust emission has different performance due to different components; The increase of DOH will lead to the increase of the manufacturing cost of the HETRTV.

(3) The simulation and test results of the HETRTV with the best mixing degree show that it can meet the driving requirements of the underground driving cycle. Compared with the WCQ-3B explosion-proof diesel engine TRTV, the dynamic performance is slightly lower, but the change is not large. The fuel consumption of the explosion-proof diesel engine and the equivalent fuel consumption of the whole vehicle are reduced by

33.9% and 12.5%, respectively. The dynamic performance and fuel economy meet the design requirements, At the same time, the emission of the exhaust gas also decreased significantly. The error of the fuel economy simulation and test is within 7%, and the exhaust emission test results are also within a reasonable range, which shows that the simulation and test results are consistent and verifies the feasibility of the design and optimization of the DOH in this paper.

Author Contributions: Data curation, investigation and writing—original draft, X.Y.; Data curation and software, Y.L.; Supervision, funding acquisition and writing—review & editing, J.B.; Methodology, P.H.; Visualization, Y.Y. and Validation, X.W. All authors have read and agreed to the published version of the manuscript.

Funding: This study was funded by the National Key Research and Development Program of China (Grant No. 2020YFB1341003), the Key Projects (Grant No. 2018-TD-ZD011) and General Projects (Grant No. 2018-TD-MS051) of China Coal Technology and Engineering Group, the Key R&D Program Projects of Shanxi Province (Grant No. 201803D121121), and the Priority Academic Program Development of Jiangsu Higher Education Institutions.

Institutional Review Board Statement: Not applicable.

Informed Consent Statement: Not applicable.

Data Availability Statement: Not applicable.

Acknowledgments: The authors wish to thank the editor and reviewers.

Conflicts of Interest: The authors declare no conflict of interest.

References

1. Varesi, K.; Radan, A.; Hosseini, S.H.; Sabahi, M. A simple technique for optimal selection of degree of hybridization (DOH) in parallel passenger hybrid cars. *Autom. J. Control. Meas. Electron. Comput. Commun.* **2015**, *56*, 33–41. [CrossRef]
2. Tan, F.; Bao, J.S.; Ge, S.R.; Yin, Y. Research status and prospects of key technologies for mine explosion-proof diesel engines. *Coal Sci. Technol.* **2018**, *46*, 176–182.
3. Maddumage, W.; Abeyasinghe, K.; Perera, M.; Attalage, R.; Kelly, P. Comparing Fuel Consumption and Emission Levels of Hybrid Powertrain Configurations and a Conventional Powertrain in Varied Drive Cycles and Degree of Hybridization. *Sci. Technol.* **2020**, *19*, 20–33. [CrossRef]
4. He, X.L.; Bao, J.S.; Yin, Y.; Ma, C. Research status of hybrid vehicle control strategy. *Mech. Transm.* **2017**, *41*, 196–200.
5. Capata, R.; Coccia, A. Procedure for the design of a hybrid-series vehicle and the hybridization degree choice. *Energies* **2010**, *3*, 450–461. [CrossRef]
6. Cui, S. Study on Parameter Matching for Hybrid Electric Vehicle Based on Electric Variable Transmission. *Trans. China Electrotech. Soc.* **2013**, *28*, 36–43.
7. Zeng, X.H.; Zhang, X.X.; Wang, W.H.; Wang, Q.N. Effect on the cost of parallel HEB for different DOH. *Trans. Chin. Soc. Agric. Mach.* **2008**, *39*, 15–19.
8. Xia, Z.A.; Gui, W.Q.; He, Z.Y.; Xue, H.Q. PHEV power transmission parameter match and optimization based on ADVISOR. *Agric. Equip. Veh. Eng.* **2015**, *53*, 22–24.
9. Hu, S.; Tang, Y.Q.; Fang, X.B. Power system match and simulation of series hybrid electric and gas of micro commercial vehicle. *Automob. Parts* **2011**, *6*, 46–49+55.
10. Han, P.X.; Bao, J.S.; Ge, S.R.; Ma, C. Parameter design of an ISG hybrid electric trackless rubber tyred vehicle based on degree of Hybridization. *Int. J. Heavy Veh. Syst.* **2017**, *24*, 239–259. [CrossRef]
11. Zeng, X.; Wang, Q.; Song, D. Simplified method to solve vehicle power demand. *J. Jilin Univ. (Eng. Ed.)* **2011**, *41*, 613–617.
12. Wang, J.M.; Guo, J.S. Power system analysis of new type hybrid bus. *Automot. Technol.* **2008**, *9*, 1–4.
13. Chen, S.Y.; Zhou, L.R.; Liu, X.W.; Chen, T.X. Exploration and practice of lead-acid batteries for electric vehicle. *Battery* **2010**, *40*, 272–275.
14. Yang, Y.X.; Cai, X.L.; Du, Q.; Liu, C.W.; Liu, J. Research on the real road emission factors and fuel consumption of typical vehicles on the roads. *J. Combust. Sci. Technol.* **2003**, *9*, 112–118.
15. Hedenus, F.; Karlsson, S.; Azar, C.; Sprei, F. Cost-effective energy carriers for transport—The role of the energy supply system in a carbon-constrained world. *Int. J. Hydrogen Energy* **2010**, *35*, 4638–4651. [CrossRef]
16. Chau, K.T.; Chan, C.C. Emerging Energy-Efficient Technologies for Hybrid Electric Vehicles. *Proc. IEEE* **2007**, *95*, 821–835. [CrossRef]
17. Zhu, Z.L.; Zhang, J.W.; Yin, C.L. Optimization approach for hybrid electric vehicle powertrain design. *Chin. J. Mech. Eng.* **2005**, *18*, 30–36. [CrossRef]

18. Wang, H.J.; Zong, C.F.; Guan, X.; Xin, R.F.; Liu, L.G. Method of Determining Weights of Subjective Evaluation Indexes for Car Handling and Stability Based on Fuzzy Analytic Hierarchy Process. *J. Mech. Eng.* **2011**, *47*, 83–90. [CrossRef]
19. Song, Z.; Zhang, X.; Li, J.; Hofmann, H.; Ouyang, M.; Du, J. Component sizing optimization of plug-in hybrid electric vehicles with the hybrid energy storage system. *Appl. Energy* **2018**, *95*, 799–804. [CrossRef]
20. Lin, X.Y.; Xue, R.; Feng, Q.G.; Zhang, S.B. Multi-objective optimization of component sizing of hybrid electric powertrain based on degree of hybridization. *J. Fuzhou Univ. (Nat. Sci. Ed.)* **2016**, *44*, 81–88.
21. Xiong, W.W.; Yin, C.L.; Zhang, Y.; Zhang, J.L. Series-parallel hybrid vehicle control strategy design and optimization using real-valued genetic algorithm. *Chin. J. Mech. Eng.* **2009**, *22*, 862–868. [CrossRef]
22. Andrade, C. Z Scores, Standard Scores, and Composite Test Scores Explained. *Indian J. Psychol. Med.* **2021**, *43*, 555–557. [CrossRef]
23. Bao, J.S.; Chen, C.; Ge, S.R.; Zhao, L.; Ma, C.; Yin, Y. Design and control strategy of distributed hybrid drive system for heavy coal trucks. *J. China Coal Soc.* **2021**, *46*, 667–676.
24. Bao, J.S.; He, X.L.; Ge, S.R.; Peng, Z.; Chen, C. Fuzzy logic control strategy for driving system of underground hybrid trackless rubber tyred vehicle. *J. China Coal Soc.* **2019**, *44*, 320–329.
25. Bian, X.; Mi, L. Development on genetic algorithm theory and its applications. *Appl. Res. Comput.* **2010**, *27*, 2425–2429.
26. Wu, G.Q.; Chen, H.Y. Multi-Objective Optimization of HEV Parameters Based on Genetic Algorithm. *Automot. Eng.* **2009**, *31*, 60–64.